

ENERGETIC ION ACCELERATION AT COLLISIONLESS SHOCKS

R. B. Decker and L. Vlahos
 The Johns Hopkins University, Applied Physics Laboratory
 Laurel, MD 20707
 USA

1. Introduction. Spacecraft observations have shown that ions are routinely accelerated to energies from ~ 10 keV to ~ 10 MeV at interplanetary shocks (1). Of particular relevance in understanding how such ion events are produced are the angle $\bar{\theta}_{Bn}$ between the mean shock normal and mean upstream magnetic field and the level of magnetic fluctuations in the shock's vicinity. When $\bar{\theta}_{Bn} \lesssim 90^\circ$ (i.e., a nearly perpendicular shock) and the magnetic field quasi-laminar, pitch angle scattering is infrequent, and ions are accelerated primarily via the scatter-free shock drift process by drifting along the $\vec{U} \times \vec{B}$ electric field parallel to the shock surface (2). When $\bar{\theta}_{Bn} \gtrsim 0^\circ$ (i.e., a nearly parallel shock) and the level of magnetic wave activity is high, pitch angle scattering is frequent, and ions are accelerated primarily via the diffusive shock acceleration process by being compressed between converging magnetic irregularities fixed in the upstream and downstream flows (3).

Although a small minority of ion events observed near 1 AU have features indicative of the acceleration process being predominantly either scatter-free shock drift or diffusive, most events are more complex, and are associated with shocks having intermediate values of $\bar{\theta}_{Bn}$ and various levels of wave activity. To model these cases, we have developed a test particle simulation that integrates along ion orbits in a system described below.

2. Model. Let $K[X,Y,Z]$ denote a system fixed with the shock, with the shock lying in the $Y-Z$ plane, and the unit vector $\hat{X} = -\hat{n}$ (\hat{n} = shock normal), so that $X < 0$ upstream (subscript 1) and $X > 0$ downstream (subscript 2). The vectors $\vec{U}_1 = U_1 (\cos \delta_1, 0, \sin \delta_1)$ and $\vec{B}_{01} = B_{01} (\cos \theta_1, 0, \sin \theta_1)$ denote the upstream plasma velocity and mean magnetic field ($\theta_1 = \bar{\theta}_{Bn}$), respectively. In K the $\vec{U} \times \vec{B}_0$ electric field is along Y . Given in addition the upstream Alfvén Mach number M_{A1} and plasma beta β_1 , the mean downstream conditions are obtained by solving the MHD jump equations (with a ratio of specific heats of 5/3).

We assume that the injected ions are true test particles (i.e., they are not coupled self-consistently to the shock and/or waves), and neglect shock structure by requiring (ion gyroradius) \gg (shock transition). Pitch angle scattering is introduced by superposing upon \vec{B}_{0i} ($i = 1$ or 2) a zero-mean, random magnetic field component $\vec{b}_i(z)$ which, in either the upstream or downstream plasma frame, varies only with coordinate z along \vec{B}_{0i} , is transverse to \vec{B}_{0i} , and is static (i.e., scattering is elastic in either plasma frame). The field $\vec{b}_i(z)$ is a superposition of N circularly polarized plane waves with wavevectors along \vec{B}_{0i} . The amplitude of each Fourier component with wavenumber k is derived from a power spectrum $P(k)$ using a well-known technique (4).

SH 1.5-3

The simulation proceeds first by constructing the $\vec{b}_1(z)$, then by solving the Lorentz force equation for the particle orbit using the field $\vec{B}_1(z) = \vec{B}_{01} + \vec{b}_1(z)$ in the appropriate plasma frame, performing a Lorentz transformation between plasma frames at shock crossings, and continuing until pre-set spatial and/or temporal boundaries are crossed, whereupon the process is repeated for a new particle.

3. Results. Acceleration at interplanetary shocks was simulated using the form $P(k)$ in Figure 1, which shows sample upstream spectra with $B_0 = B_{01} = 5$ nT. Wavenumber k in the solar wind or plasma frame (top and right axes) was related to frequency f in the spacecraft frame (bottom and left axes) via $k = 2\pi f/V_{SW}$ for a solar wind speed $V_{SW} = 4 \times 10^7$ cm/s. Spectrum A (correlation length 2×10^{11} cm) represents that of ambient transverse Alfvénic fluctuations in the interplanetary medium (5). Spectra B and C (correlation length 1.3×10^8 cm) represent transverse MHD waves presumably driven by ions streaming upstream from the shock (6,7). To model the observed spectra, we damped the upstream shock-associated field amplitude with the function $[1 + |X|/X_1^*]^{-1}$, where $X_1^* = D_1 \cos \theta_1$, with D_1 measured along \vec{B}_{01} from the shock. For $D_1 = 1.5 \times 10^{11}$ cm = 0.01 AU ($\gg 1.3 \times 10^8$ cm), the integrated power or variance σ_2^2 of C at $|X| = X_1^*$ is $0.06 B_{01}^2$, 1/4 that of spectrum B at $X = 0$, where $\sigma_2^2 = 0.25 B_{01}^2$. Downstream spectra used were similar to those in Figure 1, except $D_2 = 1.5 \times 10^{13}$ cm = 1 AU, and $\sigma_2^2 = 0.36 B_{02}^2$ to model the enhanced wave levels observed downstream of shocks. Realizations of spectra A and B for $N = 4096$ were superposed to form $\vec{b}_1(z)$, with linear interpolation used between grid points during orbit integrations. The upper scale in Figure 1 shows the resonant proton energy at which proton gyroradius $\rho \sim k^{-1}$.

Figures 2 and 3 show results for $\delta_1 = 0^\circ$, $\theta_1 = 60^\circ$, $U_1 = 4 \times 10^7$ cm/s, $B_{01} = 5$ nT, $M_{A1} = 8$, $\beta_1 = 1$, and protons injected upstream with energy $E_0 = 10$ keV in the upstream plasma frame. For this case, $B_{02}/B_{01} = 3.2$ and the plasma density jump $r = 3.7$. We define the scale time $\tau_{01} = eB_{01}/m_0c = 13$ sec (upstream proton gyroperiod) and scale length $\rho_{01} = v_0\tau_{01}/2\pi = 2.8 \times 10^8$ cm (upstream gyroradius of a 10 keV proton with speed $v_0 = 1.3 \times 10^8$ cm/s).

In Figure 2(a) kinetic energy E/E_0 in the shock frame is shown versus distance X/ρ_{01} from the shock (upstream at left, downstream at right of $X = 0$). In 2(b) and 2(c) E/E_0 and X/ρ_{01} are shown versus time t/τ_{01} during the orbit. Periods A-H in 2(a) are marked at top 2(b). The largest and most rapid

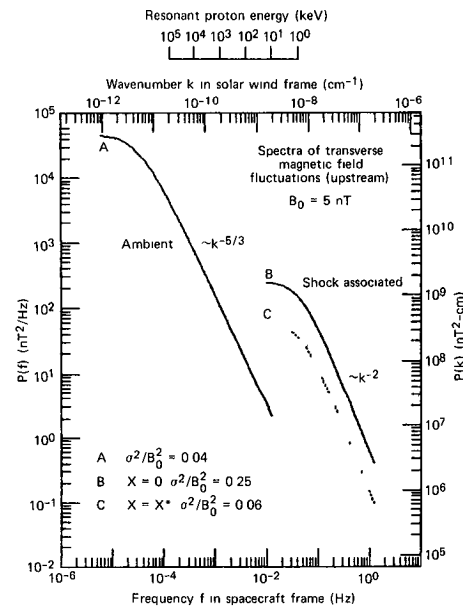


Fig. 1. Wave power spectra

SH 1.5-3

energy gains clearly occur during the shock drift phases of acceleration (e.g., $t/\tau_{01} = 8$ to 9, 11 to 14, 24 to 30, and 40 to 42). In comparison, diffusive energy gains due to compression between the inflowing upstream plasma and the shock are relatively small (e.g., $t/\tau_{01} = 14$ to 24 and 30 to 40). The particle in Figure 2 crossed the shock 42 times and was accelerated from 10 to 560 keV in $43 \tau_{01} = 9.4$ min. This orbit shows features typical of the case $\theta_1 = 60^\circ$.

In Figure 3 we show the energy spectra that result after an elapsed time of $300 \tau_{01} = 66$ min for 2900 injected protons. The quantity $\Delta f(E)/\Delta E$ is the fraction of particles with energy E within ΔE centered at the logarithmically-spaced plot points. The upstream (solid) and downstream (dashed) spectra denote sums over all particles with $X < 0$ and $X > 0$, respectively. Error bars are two statistical standard deviations in length.

4. Discussion. The most striking aspect of Figure 3 is that well-formed energy spectra spanning more than two decades in energy are produced within only one hour after injection and that these spectra bear remarkable qualitative and quantitative resemblance to observations. For example, the downstream spectrum from 10 keV to 1 MeV is well-described by a power law with spectral exponent ~ 2.2 , which is quite close to some observed values (1). In addition, the upstream

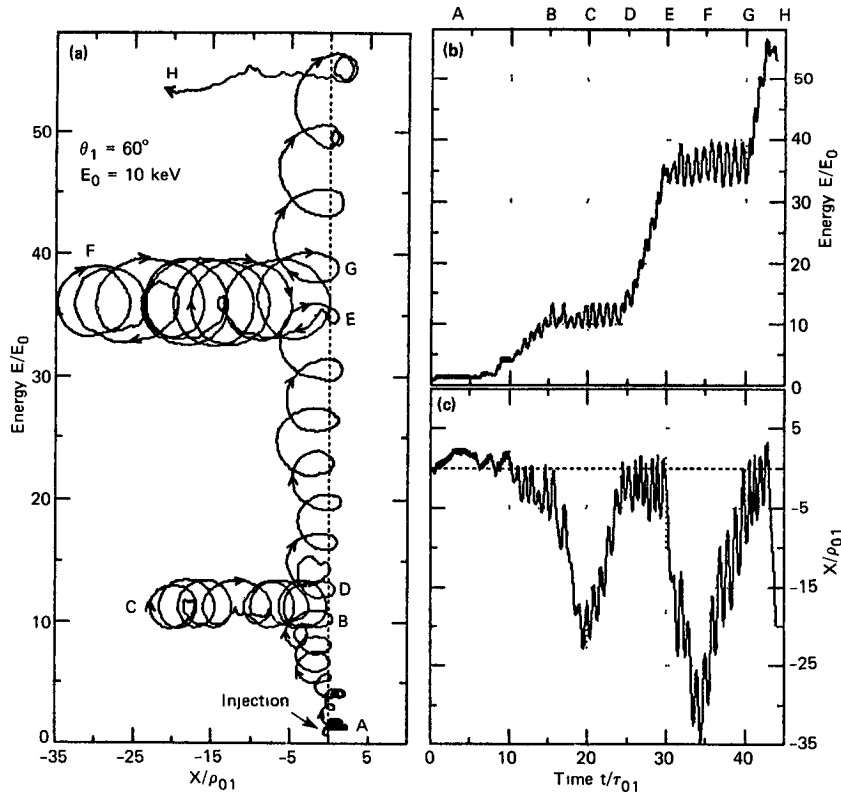


Fig. 2. Sample proton orbit

spectrum folds over with decreasing energy, similar to observed events (8). The cutoff time as well as the upstream escape boundary at $X = 0.5$ AU produce the steepening of the upstream spectrum beyond ~ 1 MeV.

We emphasize that the spectra in Figure 3 are primarily the products of the shock drift acceleration process, with pitch angle scattering simply providing the means to return particles to the shock for multiple drift acceleration phases, as in Figure 2. Diffusive acceleration contributes little to acceleration in this case. To estimate the maximum effect expected from diffusive acceleration, we set $\theta_1 = 0^\circ$, and keeping all other parameters fixed as in the $\theta_1 = 60^\circ$ case, injected particles at 10 keV ($B_{02}/B_{01} = 1$ and $r = 3.85$ in this case). After $300 \tau_{01}$ the spectra extended no further than $E/E_0 = 10$ or 100 keV, illustrating, as one might expect, that 300 gyroperiods is far too short a period for diffusive acceleration alone to produce an extended energy spectrum. Examples of energy spectra for various values of θ_1 from 0° to 75° are shown by reference 9.

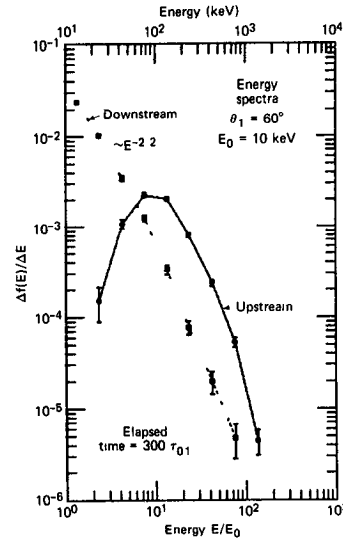


Fig. 3. Proton energy spectra

5. Conclusions. We have presented an example from a test particle simulation designed to study ion acceleration at oblique turbulent shocks. For conditions appropriate at interplanetary shocks near 1 AU, we have found that a shock with $\theta_{Bn} = 60^\circ$ is capable of producing an energy spectrum extending from 10 keV to ~ 1 MeV in ~ 1 hour. In this case total energy gains result primarily from several separate episodes of shock drift acceleration, each of which occurs when particles are scattered back to the shock by magnetic fluctuations in the shock vicinity.

6. Acknowledgements. This work was supported in part by the JHU/APL Independent Research and Development Program under Navy Contract N00024-83-C-5301 and in part by NSF Grant ATM-83-05537.

References

1. van Nes, P., et al.: 1984, JGR, 89, 2122.
2. Decker, R. B.: 1983, JGR, 88, 9959.
3. Lee, M. A.: 1983, JGR, 88, 6109.
4. Owens, A. J.: 1978, JGR, 83, 1673.
5. Hedgecock, P. C.: 1975, Solar Phys., 42, 497.
6. Tsurutani, B. T., et al.: 1983, JGR, 88, 5645.
7. Sanderson, T. R., et al.: 1985, JGR, 90, 3973.
8. Decker, R. B., et al.: 1981, JGR, 86, 8819.
9. Decker, R. B. and Vlahos, L.: 1985, paper SH 1.1-6, these proceedings.